



HAL
open science

A detonation run-up distance database: data-driven existing models improvement and new model development

Cristian Mejía-Botero, Florent Viot, Luís Fernando Figueira da Silva, J. Melguizo-Gavilanes

► To cite this version:

Cristian Mejía-Botero, Florent Viot, Luís Fernando Figueira da Silva, J. Melguizo-Gavilanes. A detonation run-up distance database: data-driven existing models improvement and new model development. 2024. hal-04417228v2

HAL Id: hal-04417228

<https://hal.science/hal-04417228v2>

Preprint submitted on 17 Jun 2024

HAL is a multi-disciplinary open access archive for the deposit and dissemination of scientific research documents, whether they are published or not. The documents may come from teaching and research institutions in France or abroad, or from public or private research centers.

L'archive ouverte pluridisciplinaire **HAL**, est destinée au dépôt et à la diffusion de documents scientifiques de niveau recherche, publiés ou non, émanant des établissements d'enseignement et de recherche français ou étrangers, des laboratoires publics ou privés.

A detonation run-up distance database: data-driven existing models improvement and new model development

C. Mejía-Botero^{a,*}, F. Virost^a, L.F. Figueira da Silva^a, J. Melguizo-Gavilanes^{a,b}

^a Institut Pprime, CNRS, ISAE-ENSMA, Université de Poitiers, BP 40109, 86961 Futuroscope-Chasseneuil Cedex, France
^b Shell Global Solutions B.V., Major Hazards Management, Energy Transition Campus, 1031 HW Amsterdam, The Netherlands

Abstract

A comprehensive database of detonation run-up distances (x_{DDT}) in unobstructed tubes/channels is compiled. Eight fuels are included, i.e., hydrogen, methane, ethane, ethylene, acetylene, propane, butane and carbon monoxide. Oxygen is used as oxidizer with different diluents under a wide range of tube/channel sizes. In total 559 points are collected and analyzed. The global x_{DDT} trends observed in the data as a function of the initial conditions (i.e., fuel type, equivalence ratio (ϕ), hydraulic diameter (D_h), and pressure (p)) reveal that x_{DDT} decreases with increasing p , decreasing D_h , and $\phi \rightarrow 1$. The correlation of the normalized run-up distance x_{DDT}/D_h with geometrical parameters and fundamental combustion properties shows that most of the variance in the experimental data can be captured by the ratio of D_h to the flame thickness (D_h/δ_f), the expansion ratio ($\sigma - 1$) and that of the Chapman-Jouguet to the laminar flame speed ($V_{CJ}/\sigma s_L$). With these, a non-linear (NLM) and a logarithmic model (LM) are proposed using a non-linear least squares regression to fit a user-defined function. The NLM and LM are shown to outperform the widely used Silvestrini and Dorofeev models by a large margin since they are capable of explaining $\sim 70 - 80\%$ of the variance in the experimental x_{DDT}/D_h data in contrast to only $\sim 20\%$ of the original Silvestrini and Dorofeev models. The poor performance of the original models is due to the limited amount of data used to determine the models constants. An update to these constants is also carried out using the database collected in this work resulting in a notable improvement of their predictive capabilities over the original models. The database is publicly available so that it can be used freely to guide future research in the combustion community (e.g., by identifying conditions where there is a lack of data), and as a test bed for further data-driven model development.

Keywords: Deflagration-to-detonation transition; detonation run-up distances; data-driven models; flame acceleration; fuel safety

1. Introduction

Under certain conditions, after accidental ignition of a reactive cloud, the initial flame may accelerate and transit to detonation, the so-called, deflagration-to-detonation-transition (DDT) phenomenon. Detonation is a supersonic combustion propagation regime that is much stronger and more destructive than a flame. Although in most cases DDT occurs due to flame/shock/obstacles interactions, it can also occur in unobstructed spaces, such as gas compartments and hoses in fuel cells, battery packs, electrolyzers, among others. The determination of the DDT run-up distance x_{DDT} , defined as the distance between ignition of the flame and detonation onset, is not only important for safety but also for the optimal design of pulse detonation engines (PDE) [1].

One way to estimate x_{DDT} is by using experimental data together with phenomenological models. For the latter, those proposed by Silvestrini et al. [2] and Dorofeev et al. [3] are the most widely used for predicting x_{DDT} in unobstructed channels. In [2] an expression for x_{DDT}/D_h is proposed, where D_h is the hydraulic diameter of the tube/channel; hereinafter, the word channel(s) will be used to refer to either. The model assumes that the flame: (i) is ignited at the closed end and propagates towards the open end; (ii) its speed, V_F , increases exponentially with the relative axial position of the channel, x/D_h , i.e., $V_F = A\sigma s_L \exp[B(\sigma - 1)(x/D_h)(D_h/D_{ref})^n]$, where s_L is the laminar flame speed, σ is the expansion ratio, D_{ref} is a reference diameter, and A, B, and n are constants.

To estimate the constants, six $V_F(x)$ experimental data for hydrogen, propane, and ethylene in air [4, 5] were used. These tests were performed in 150, 250, and 1400 mm diameter channels. Only one $V_F(x)$ profile per mixture was considered during curve fitting. The criterion to predict x_{DDT}/D_h is that V_F must achieve a critical value suitable to trigger DDT, that is, half of the Chapman–Jouguet detonation velocity, $V_F = V_{CJ}/2$. Silvestrini’s model is thus

$$\frac{x_{DDT}}{D_h} = \frac{1}{B(\sigma - 1)} \left(\frac{D_{ref}}{D_h} \right)^n \ln \left(F \frac{V_{CJ}}{\sigma s_L} \right), \quad (1)$$

where $B = 0.0061$, $n = 0.4$, $D_{ref} = 0.15$ m, and $F = 0.5/A = 0.077$. Since the constants were not determined directly using x_{DDT} data but with $V_F = f(x)$ profiles, the model prediction is limited by the $V_F = V_{CJ}/2$ assumption.

On the other hand, the model proposed in [3] is derived via a mass balance considering that the flame propagation speed is affected by the hydrodynamic boundary layer (BL) growth in the channel whose relative thickness is denoted by Δ . To estimate Δ , the BL is assumed to grow linearly with the channel’s wall roughness, d and axial position, x , i.e., $x/\Delta = [\ln(\Delta/d)/\kappa + K]/C$, where C , κ and K are constants. x_{DDT}/D_h is obtained upon substitution of the latter expression into the mass balance, and as-

suming that DDT occurs when V_F reaches the sound speed in burnt gases, i.e., $V_F = c_b$. Dorofeev’s model is

$$\frac{x_{DDT}}{D_h} = \frac{\Gamma}{C} \left[\frac{1}{\kappa} \ln \left(\Gamma \frac{D_h}{d} \right) + K \right], \quad (2)$$

$$\text{where } \Gamma = \left[\frac{c_b}{\zeta(\sigma - 1)^2 s_L} \left(\frac{\delta_f}{D_h} \right)^\xi \right]^{\frac{1}{2m+7/3}},$$

and $\delta_f = \alpha/s_L$ is the laminar flame thickness with α denoting the mixture thermal diffusivity; ζ and m are additional constants. To estimate the constants, nine $V_F(x)$ data from [6–10] were used, of which eight were H₂-O₂/air mixtures, and one a hydrocarbon (HC)/air mixture. Four of these were performed using channels with blockage ratio ≈ 0.1 , which is known to modify the DDT behavior compared with unobstructed channels. The D_h range considered was $D_h \in [15, 520]$ mm resulting in $C = 0.2$, $\kappa = 0.4$, $K = 5.5$, $\zeta = 2.1$, $\xi = 1/3$ and $m = -0.18$.

It is evident that the models performance hinges on the appropriate determination of the constants. The limited data used in [2] and [3] did not account for a wide range of fuels, diluents, compositions/equivalence ratios (ϕ) and D_h , so their predictions are expectedly restricted. Indeed in [11], Silvestrini’s model was evaluated against data from [12, 13] showing poor performance for all the experimental conditions tested. For DDT predictions, large amounts of data are required to account for the variability of the process.

To fill this gap, here, a large database is compiled using all the x_{DDT} data for unobstructed channels available in the literature. In total, 559 tests were collected, including both HCs and hydrogen over a wide range of experimental conditions (D_h , ϕ , pressure (p) and temperature (T)). The constants of the Silvestrini and Dorofeev models are updated resulting in a significant improvement of their predictive capabilities. Furthermore, two additional simpler expressions that outperform the original Silvestrini and Dorofeev models by a large margin are proposed.

2. Database description

To collect the data a systematic search was performed in *Scopus*. As criteria, only scientific papers reporting experimental x_{DDT} values obtained in unobstructed channels using weak ignition sources to avoid direct detonation initiation were considered. x_{DDT} is compiled together with the mixture initial conditions, i.e., T , p , and ϕ . Geometrical information such as D_h , length (L), cross-section (CS) and boundary conditions (BC) are also included. The latter refers to channels with Closed/Closed (C/C) or Closed/Opened ends (C/O). Table 1 summarizes the data collected. A total of 36 references were reviewed. The data are split into C/O and C/C channels, and ordered according to the fuel used. Experi-

1 mental data obtained for the current work in the two-
 2 directional schlieren visualization set-up described in
 3 [14, 15] are included as well.

4 2.1. Geometrical parameters

5 The ranges of L and D_h for which data were found
 6 are $L \in [0.4, 40]$ m and $D_h \in [0.6, 406]$ mm, and
 7 $L \in [0.8, 24]$ m and $D_h \in [0.5, 159]$ mm for C/O
 8 and C/C channels, respectively. The minimum and
 9 maximum L/D_h ratios in the dataset are $L/D_h = 6$
 10 and 4000.

11 2.2. Mixtures and initial conditions

12 A total of eight fuels are included, i.e., hydro-
 13 gen (H_2), methane (CH_4), ethane (C_2H_6), ethylene
 14 (C_2H_4), acetylene (C_2H_2), propane (C_3H_8), butane
 15 (C_4H_{10}), and carbon monoxide (CO). Almost all are
 16 fuels of a single component, except for some in [30]
 17 that correspond to CH_4/C_2H_6 , some in [26] that used
 18 H_2/C_3H_8 , and some measured by the current authors
 19 using H_2/CH_4 blends. Oxygen (O_2) is the oxidizer
 20 whereas nitrogen (N_2), helium (He), argon (Ar) and
 21 carbon dioxide (CO_2) are used as diluents. The initial
 22 conditions ranges are $T \in [298, 473]$ K, $p \in$
 23 $[0.1, 25]$ bar, and $\phi \in [0.2, 5.8]$.

24 2.3. Number of data points and distribution

25 Table 1 also shows the number of data points (DP)
 26 per fuel. 202 and 357 DP were collected for C/O and
 27 C/C which correspond to a total of 559 tests. H_2 and
 28 C_2H_4 are the most often used fuels, with 193 and 191
 29 DP, respectively. These are followed by C_3H_8 (95
 30 DP), and CH_4 (29 DP). The least used are C_2H_2 (18
 31 DP), CO (15 DP), C_2H_6 (9 DP), and C_4H_{10} (9 DP).

32 Figure 1 shows the D_h , Φ and p histograms for
 33 (a) C/O, and (b) C/C. Tests carried out with H_2 and
 34 HC are plotted with different colors; the 15 DP with
 35 CO are not included. The histograms reveal that for
 36 both BCs most of the tests were performed in chan-
 37 nels with $D_h \leq 50$ mm.

38 Regarding mixture compositions, the normalized
 39 equivalence ratio, $\Phi = \phi/(1 + \phi)$ is used to center
 40 the distribution at $\phi = 1.0$ (i.e., $\Phi = 0.5$), thereby
 41 lengthening the axis for $\phi < 1$ and shortening it for
 42 $\phi > 1$. For C/O, most of the tests are performed with
 43 HC fuels of which 81 DP correspond to stoichiometric
 44 ($\Phi = 0.5$), 28 to lean ($\Phi < 0.5$), and 37 to rich
 45 ($\Phi > 0.5$) conditions. For H_2 , 29 DP correspond to
 46 $\Phi = 0.5$, 11 to $\Phi < 0.5$, and 16 to $\Phi > 0.5$. For C/C,
 47 the data is distributed as follows: 171 DP at $\Phi = 0.5$,
 48 14 at $\Phi < 0.5$, and 20 at $\Phi > 0.5$ for HC mixtures.
 49 For H_2 mixtures, 81 DP correspond to $\Phi = 0.5$, 29
 50 to $\Phi < 0.5$, and 27 to $\Phi > 0.5$. Finally, the p
 51 histogram shows, expectedly, that all the tests with C/O
 52 channels are performed at atmospheric pressure, i.e.,
 53 $p \approx 1$ bar. For C/C, most of the tests are carried out
 54 at $p < 1$ bar with 157 and 14 DP for HC and H_2 mix-
 55 tures, respectively. For $p > 1.0$ bar, 21 (HC) and 92

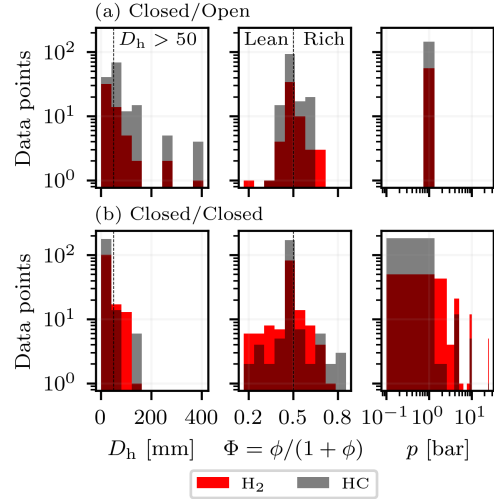


Fig. 1: Histograms for D_h , Φ and p . (a) Closed/Open; (b) Closed/Closed channels.

56 (H_2) DP were found, and at $p = 1.0$ bar, 27 (HC) and
 57 31 (H_2) DP were collected

58 This visualization allows to identify regions where
 59 there is little to no data available in the literature, and
 60 may serve as a guide for future DDT research. As an
 61 example, only 9 data points were collected at 473 K
 62 for C/C channels [22]. The remaining were obtained
 63 at room temperature, i.e., ≈ 298 K (not shown). This
 64 shows high research potential of the effect of T on
 65 x_{DDT} in unobstructed channels since most of the in-
 66 dustrial processes where DDT may occur are either
 67 at high T , e.g., electrolyzers and nuclear reactors, or
 68 low T , e.g., cryogenic fuel or oxidizer transportation.
 69 Additionally, the lack of data for $D_h > 50$ mm is
 70 evident, which corresponds to most of the industrial
 71 pipelines in service. Data is missing for C_2H_2 , C_2H_6 ,
 72 and C_4H_{10} , HC extensively used in many industries.
 73 Likewise for CO, which is of interest because it is one
 74 of the main components of Syngas and it is expected
 75 to play an important role in the energy transition. Fi-
 76 nally, note that most data exist at stoichiometric con-
 77 ditions but many accidents are the result of accidental
 78 ignition of a reactive cloud after leakage/mixing of
 79 fuel/oxidizer effectively resulting in scenarios where
 80 lean/rich mixtures are present.

81 2.4. Preprocessing of database

82 Three conditions were identified for which the
 83 DP follow different trends compared to most of the
 84 tests in the database: (i) channels with $D_h < 3$ mm;
 85 123 DP from [23–25, 33–35, 41, 42]. These include
 86 tests with both H_2 and HC for C/O and C/C at
 87 $\phi \in [0.7, 1.7]$, and $p \in [0.1, 2.4]$ bar performed
 88 mostly in spiral channels or with central ignition.
 89 (ii) channels with non-unity aspect ratio (AR); 119
 90 DP from [27, 36] with AR ranging from 1:1.5 to

Table 1: Database summary.

Fuel	BC	ϕ	Diluents	D_h [mm]	L [m]	p [bar]	CS	DP	References
H ₂	C/O	0.25 – 2.1	N ₂ , Ar, He	3 – 406	1 – 40	1	Cir.; Sqr.	56	[5, 11, 12, 14, 16–21], CW
	C/C	0.2 – 2.8	N ₂ , Ar, He, CO ₂	0.5 – 159	0.8 – 24	0.1 – 25	Cir.; Rec.	137	[6, 7, 13, 22–29]
CH ₄	C/O	1.0	N ₂	10 – 50	1 – 11	1	Cir.; Sqr.	12	[11, 15, 18, 30], CW
	C/C	0.35 – 2.0	N ₂	15 – 20	1.5 – 2.9	0.3 – 25	Cir.; Sqr.	17	[22, 31]
C ₂ H ₂	C/O	–	–	–	–	–	–	–	–
	C/C	0.27 – 5.8	N ₂	15	2.9	1 – 5	Cir.	18	[22]
C ₂ H ₄	C/O	0.63 – 1.7	N ₂	0.6 – 406	0.4 – 40	1	Cir.; Sqr.	55	[5, 11, 18, 32–35]
	C/C	0.35 – 2.7	N ₂	10 – 127	1 – 6	0.1 – 1.7	Cir.; Rec.	136	[7, 28, 36–39]
C ₂ H ₆	C/O	1.0	N ₂	26 – 50	2 – 11	1	Cir.	9	[18, 30]
	C/C	–	–	–	–	–	–	–	–
C ₃ H ₈	C/O	0.5 – 1.7	N ₂	25.4 – 406	0.5 – 40	1	Cir.	61	[5, 11, 30, 32, 40]
	C/C	1.0	N ₂	0.5 – 3	2	0.1 – 1	Cir.	34	[26, 41]
C ₄ H ₁₀	C/O	1.0	N ₂	50.8	11	1	Cir.	9	[30]
	C/C	–	–	–	–	–	–	–	–
CO	C/O	–	–	–	–	–	–	–	–
	C/C	0.4 – 2.0	–	50	2.9	5 – 25	Cir.	15	[22]

Legend: current work (CW); circular (Cir.); square (Sqr.); rectangular (Rec.). Refs. [27, 36] include channels with AR $\neq 1$.

1:30. These include tests with stoichiometric H₂ and C₂H₄ at $p < 0.7$ bar. (iii) the use of CO as fuel, with 15 DP from [22]; these tests were carried out at high pressure, i.e., $p \in [5 - 25]$ bar. Only data that did not meet the conditions above are considered in the analysis that follows. A total of 302 DP are thus retained after filtering: 132 for H₂ and 170 for HC mixtures. The final experimental ranges are $D_h \in [3, 406]$ mm, $\phi \in [0.2, 5.8]$, $p \in [0.12, 25]$ bar, and $T \in [298, 474]$ K.

The database and scripts are made publicly available as a github repository (<https://github.com/MejiaBotero/DDTdatabase>).

3. x_{DDT} trends

3.1. x_{DDT} vs. D_h , Φ , and p

It is of practical interest (safety/propulsion) to identify/verify the general dependence of x_{DDT} on geometrical and initial conditions. Figure 2 shows these trends as a function of D_h , Φ , and p . For ease of visualization, selected cases were taken from the database to isolate the effect of the respective variable on x_{DDT} , however, the trends hold for all mixtures considered. Concerning D_h , stoichiometric ($\Phi = 0.5$) H₂/air and C₂H₄/air at $p = 1$ bar from [5, 16, 32]. The plot shows that x_{DDT} increases almost linearly with D_h for both mixtures. Regarding Φ , H₂/air and C₃H₈/air mixtures from [16, 32] tested in $D_h = 50$ mm channels at $p = 1$ bar. A U-shape curve is observed with x_{DDT} exhibiting a minimum around $\Phi = 0.5$. Finally for p , part of the experiments presented in [22] for H₂/O₂ and CH₄/O₂ in $D_h = 15$ mm channels at $\Phi = 0.5$ are shown. There is a pronounced decrease

in x_{DDT} as p increases. The trends reveal that the use of pure O₂ as oxidizer significantly decreases x_{DDT} for H₂ and HC mixtures. Based on the database collected, for PDE design where short x_{DDT} values are desirable, small D_h channels at high pressure and under stoichiometric conditions using pure O₂ as oxidizer are advised; the opposite holds for safety applications.

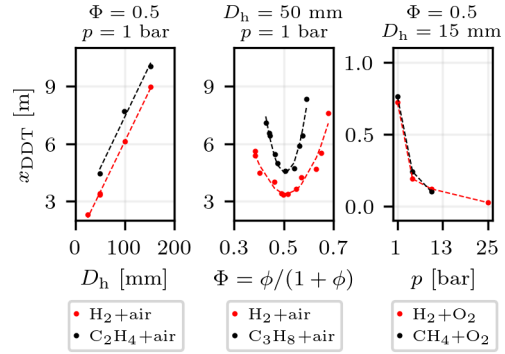


Fig. 2: x_{DDT} trends vs. D_h , Φ , and p for selected cases.

3.2. x_{DDT}/D_h vs. fundamental combustion properties

The effect on x_{DDT} of the (ratios of) fundamental combustion properties (i.e., V_{C1}/σ_{sL} , c_b/s_L , and $\sigma - 1$) and that of the channel size to the laminar flame thickness (i.e., D_h/δ_f) used in the Silvestrini and Dorofeev models is evaluated next to assess whether the dependencies assumed hold, and to identify potentially overlooked relevant variables. The analysis is carried out on x_{DDT}/D_h to absorb channel size effects

1 on the output variable. The hydraulic diameter to deto- 42
 2 onation induction length ratio, D_h/l_{ind} , the Zel'dovich 43
 3 number, $\beta = E_a(T_b - T_u)/(RT_b^2)$, and the heat capa- 44
 4 city ratio, $\gamma = c_p/c_v$, are also evaluated. E_a is the 45
 5 effective activation energy, T_b and T_u are the burnt 46
 6 and unburnt/fresh gases temperature, respectively; c_p 47
 7 and c_v are the heat capacity at constant pressure and 48
 8 volume. All properties were computed with Cantera 49
 9 using GRI 3.0 chemical mechanism, except for 50
 10 C_4H_{10} for which the San Diego mechanism was used. 51
 11 Figure 3 shows the Pearson autocorrelation matrix for 52
 12 the properties considered which measures colinearity 53
 13 between two sets of data. Values close to unity indicate 54
 14 a strong correlation, and suggest that these variables 55
 15 capture the x_{DDT}/D_h dependencies observed in 56
 16 the data.

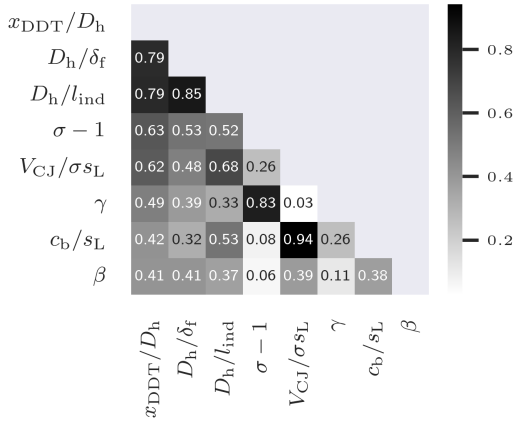


Fig. 3: Pearson autocorrelation matrix for x_{DDT}/D_h .

17 The most correlated with x_{DDT}/D_h are D_h/δ_f and 18
 19 D_h/l_{ind} , both with correlation coefficients of 0.79. 20
 21 Note however that these two variables are also correlated 22
 22 with each other indicating that they provide similar 23
 23 statistical information about x_{DDT}/D_h . D_h/δ_f is 24
 24 retained since for flame propagation and acceleration 25
 25 δ_f is a more sensible length scale to consider. Notably, 26
 26 the latter ratio is included in Dorofeev's and not in 27
 27 Silvestrini's model. The next in line is $\sigma - 1$ which 28
 28 was found to have a strong effect on the x_{DDT}/D_h 29
 29 predictions that will be presented in section 5, and to be 30
 30 highly correlated to γ ; both Silvestrini and Dorofeev 31
 31 include $\sigma - 1$ and omit γ in their models. The fol- 32
 32 lowing is V_{CJ}/σ_{sL} (used in Silvestrini) which in turn 33
 33 is correlated to c_b/s_L (used in Dorofeev). The former 34
 34 ratio is retained because of its higher correlation with 35
 35 x_{DDT}/D_h . In addition, β exhibits a correlation coeffi- 36
 36 cient of 0.41. While similar to that of c_b/s_L , it does 37
 37 not seem to be correlated to any of the other variables 38
 38 considered. The addition of this property to the models 39
 39 proposed in section 5 had a very modest effect on their 40
 40 performance, consequently, it was not considered further. 41
 41 Finally, the high correlations between (i) V_{CJ}/σ_{sL} and c_b/s_L , and (ii) D_h/δ_f and D_h/l_{ind} , are worth mentioning. While (i) is not surprising because

42 $c_b \approx V_{CJ}/2$, (ii) is not so straightforward since these 43
 44 two lengths are governed by different physics. The latter 45
 45 observation may warrant a deeper analysis but it is beyond 46
 46 the scope of the current work.

47 Figure 4 shows the trends of x_{DDT}/D_h with D_h/δ_f , 48
 49 V_{CJ}/σ_{sL} , and $\sigma - 1$. The BC type does not seem to 49
 50 have an important effect on x_{DDT}/D_h since both 51
 51 C/O and C/C follow the same behavior. D_h/δ_f is in- 52
 52 versely proportional to x_{DDT}/D_h . Large D_h/δ_f values 53
 53 indicate that the flame is thin compared to the channel 54
 54 dimensions, which in turn favors the development of 55
 55 surface instabilities and large flame surface area. This 56
 56 results in increased flame acceleration leading to a decrease 57
 57 in x_{DDT}/D_h . On the other hand, x_{DDT}/D_h is directly 58
 58 proportional to V_{CJ}/σ_{sL} . A mixture with high V_{CJ} must 59
 59 be accelerated more prior to transition, and a low σ_{sL} is 60
 60 representative of mixtures with slow laminar flame speeds. 61
 61 It is thus expected that a large V_{CJ}/σ_{sL} ratio results in 62
 62 large x_{DDT}/D_h values. Finally, of interest is that $\sigma - 1$, 63
 63 exhibits different slopes for H_2 and HC while both being 64
 64 inversely proportional to x_{DDT}/D_h . The latter observation 65
 65 stems from the fact that there is a large difference in σ 66
 66 between both fuel types. For the conditions at hand (i.e., 67
 67 flame acceleration in channels ignited at the closed end), 68
 68 higher σ values lead to increased acceleration rates during the early stages of flame propagation.

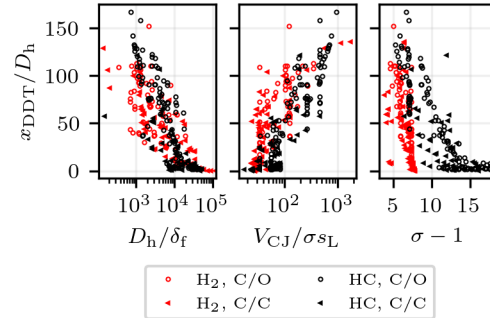


Fig. 4: x_{DDT}/D_h vs. ratios of fundamental combustion properties.

4. Existing model evaluation

4.1. Silvestrini and Dorofeev vs. database

71 Figure 5 compares the models predictions against the 72
 72 experimental database. A 45° line showing the ideal 73
 73 performance is added as a visual aid. That is, values that 74
 74 are predicted well by the models are expected to fall on 75
 75 this line. Most references do not report the standard deviation 76
 76 of their x_{DDT} data, hence an arbitrarily defined deviation 77
 77 band of $\pm 15\%$ (blue shading) is plotted to account for 78
 78 experimental uncertainties. The coefficient of determination (R^2) 79
 79 is used as our metric to assess the models performance. It was 80
 80 computed using standard functions from the scikit-learn 81
 81 package [43]. The best possible score is $R^2 = 1$ 82

1 and it can be negative. A negative R^2 implies that a
 2 model fits the data worse than a horizontal line at a
 3 height equal to the mean of the observed data. This
 4 occurs when a wrong model is chosen or nonsensical
 5 constraints are inadvertently applied.

6 Both models performed poorly with R^2 of -0.88
 7 and 0.23 for Silvestrini and Dorofeev, respectively.
 8 R^2 was also computed for H_2 and HC mixtures sepa-
 9 rately. The scatter is higher for H_2 mixtures ($R_{H_2}^2 =$
 10 -3.5 (Silvestrini) and -0.05 (Dorofeev)) than with
 11 HCs ($R_{HC}^2 = 0.54$ (Silvestrini) and 0.37 (Dorofeev)).
 12 Note that there are *outliers* present in the evalua-
 13 tion of the models. These are simply a reflection of
 14 their (poor) performance against our database, and
 15 a consequence of the limited amount of data used
 16 to determine the original models constants. Ulti-
 17 mately, this prevents them from properly reproduc-
 18 ing the x_{DDT}/D_h trends with fundamental combus-
 19 tion properties over the wide range of experimental
 20 conditions considered. In subsection 4.2 the original
 21 constants are updated.

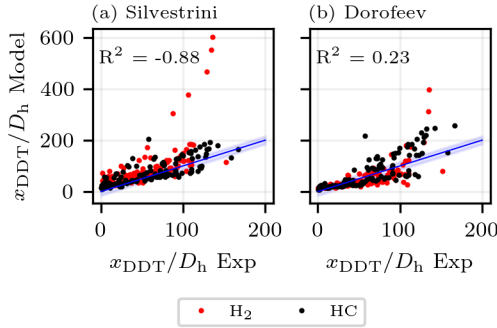


Fig. 5: Original models performance against database: a) Silvestrini and b) Dorofeev.

22 4.2. Updated Silvestrini and Dorofeev constants

23 An update to Silvestrini and Dorofeev model constants
 24 was done using the database collected in this
 25 work which includes a much wider range of operat-
 26 ing conditions and fuels. As the fitting target is
 27 x_{DDT} rather than $V_F = f(x)$ data, it allows for
 28 a direct prediction/estimate of the variable of inter-
 29 est. 80 % of the data were used as the training
 30 set and 20 % as the test set. That is, 242 DP
 31 were used to determine the constants and 60 DP to
 32 evaluate the performance of the models. To select
 33 these data, the *train_test_split()* function of scikit-
 34 learn [43] was used. It splits the data randomly
 35 by selecting a user-defined percentage. The initial
 36 conditions ranges for the training data are $D_h \in$
 37 $[3, 406]$ mm, $\phi \in [0.2, 5.8]$, $p \in [0.12, 25]$ bar,
 38 and $T \in [298, 474]$ K, and for the test data $D_h \in$
 39 $[3, 406]$ mm, $\phi \in [0.21, 2.8]$, $p \in [0.21, 25]$ bar, and
 40 $T \in [298, 474]$ K. The fitting was carried out using
 41 the *optimize.curve_fit()* function of SciPy which

42 essentially uses a non-linear least squares regression
 43 method to fit a function. The updated constants are
 44 listed in Table 2.

45 Figure 6 shows the fitting results with the training
 46 data and the performance with the test data for the
 47 updated a) Silvestrini, and b) Dorofeev. The improve-
 48 ment is evident with R^2 values of 0.74 and 0.73
 49 for the respective models with the train data. Their
 50 performance with the test data have R^2 values of 0.7
 51 and 0.71 , respectively. Again, this represents signifi-
 52 cant improvements compared to the original models,
 53 and indicates that $\sim 70\%$ of the variance in x_{DDT}/D_h
 54 can now be explained by the updated models. The re-
 55 maining $\sim 30\%$ can be attributed to unknown lurking
 56 variables or inherent variability. Note that the model's
 57 underlying assumptions were carefully verified to en-
 58 sure that the updated constants values did not lead to
 59 non-physical flame velocities (Silvestrini) or unrea-
 60 sonable BL growth (Dorofeev) as a function of the
 61 axial position in the channel. Silvestrini/Dorofeev re-
 62 sulted in a measurable/modest increase/decrease com-
 63 pared to that originally obtained. The revised $V_F(x)$
 64 and $\Delta(x)$ dependence better reflects the experimen-
 tally observed trends (not shown).

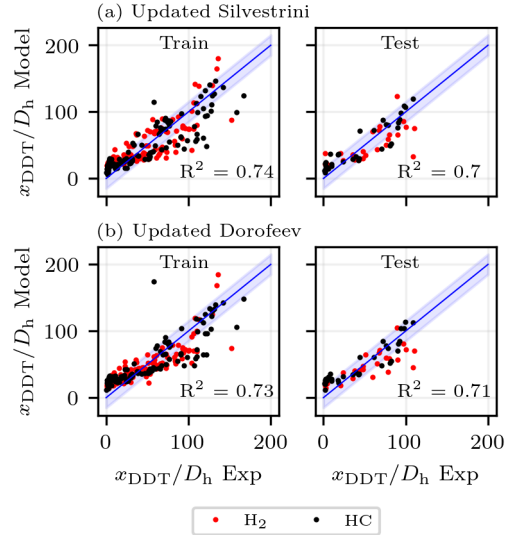


Fig. 6: Updated a) Silvestrini and b) Dorofeev performance for training and test data.

5. Proposed models

67 Two additional simpler models are proposed, i.e.,
 68 non-linear (NLM) and logarithmic (LM), that lever-
 69 age the learnings from the data analysis carried out in
 70 the previous sections. The expressions are shown in
 71 Equation 3, and Equation 4, respectively.

$$\frac{x_{DDT}}{D_h} = \frac{a_0}{(\sigma - 1)^{a_1}} \left(\frac{D_h}{\delta_f} \right)^{-a_2} \left(\frac{V_{Cl}}{\sigma_{SL}} \right)^{a_3}, \quad (3)$$

$$\frac{x_{DDT}}{D_h} = \frac{b_0}{(\sigma - 1)^{b_1}} \ln \left[b_2 \left(\frac{D_h}{\delta_f} \right)^{-1} \left(\frac{V_{CJ}}{\sigma s_L} \right) \right]. \quad (4)$$

1 NLM considers the influence of the most important
 2 variables discussed in subsection 3.2 to estimate four
 3 constants: a_0 , a_1 , a_2 , and a_3 . Note that this expres-
 4 sion is general and does not take into account any in-
 5 formation regarding the x_{DDT}/D_h trends observed in
 6 Figure 4. On the other hand, LM accounts for the log-
 7 arithmic trend that x_{DDT}/D_h exhibits when plotted as
 8 a function of D_h/δ_f and $V_{CJ}/\sigma s_L$. Three constants
 9 need being estimated: b_0 , b_1 , and b_2 . The constraint
 10 $b_2 > (D_h/\delta_f)(V_{CJ}/\sigma s_L)^{-1}$ was enforced during the
 11 regression so that the argument of the natural loga-
 12 rithm is always greater than unity thereby ensuring
 13 that all the x_{DDT}/D_h estimates are positive; Table 2
 14 lists the fitting results. Note that although these are
 15 data driven models, the choice of variables is based
 16 on lower/upper bounds for combustion wave steady
 17 propagation speeds (i.e., s_L and V_{CJ}), length scales
 18 (i.e., δ_f and D_h), first order approximations of the
 19 flow induced ahead of the flame (i.e., $(\sigma - 1)s_L$),
 20 and the flame speed in the laboratory frame (i.e.,
 21 $V_F = \sigma s_L$). All of them have physical significance
 22 and are relevant to the FA process. Therefore, these
 23 are semi-empirical models that take into account the
 24 phenomenology of the process.

Table 2: Models constants.

Model	Eq.	Constants	
		Original	Updated
Silvestrini	eq. (1)	$B = 0.0061$	$B' = 0.0057$
		$n = 0.4$	$n' = 0.07$
		$F = 0.077$	$F' = 0.084$
		$C = 0.2$	$C' = 0.26$
Dorofeev	eq. (2)	$\kappa = 0.4$	$\kappa' = 0.13$
		$K = 5.5$	$K' = -1.75$
		$\zeta = 2.1$	$\zeta' = 0.046$
		$\xi = 1/3$	$\xi' = 1.32$
		$m' = -0.18$	$m' = 1.46$
NLM	eq. (3)	$a_0 = 184$	
		$a_1 = 0.82$	
		$a_2 = 0.11$	
		$a_3 = 0.29$	
LM	eq. (4)	$b_0 = 50$	
		$b_1 = 0.7$	
		$b_2 = 4500$	

25 Figure 7 shows the fitting with the train, and the
 26 evaluation with the test data for a) NLM, and b) LM.
 27 Both train and test data are the same sets used in the
 28 previous sections to enable a meaningful comparison
 29 of the models performance. The LM has a better fit to
 30 the training data with an R^2 of 0.78 compared to 0.72
 31 for the NLM. This was also reflected in the perfor-
 32 mance with the test data, with a R^2 of 0.84 for the LM

33 and 0.74 for the NLM. The prediction of both mod-
 34 els is much better than that of the original Dorofeev
 35 and Silvestrini, and have higher (LM)/similar (NLM)
 36 R^2 values than those obtained with the updated Sil-
 37 vestrini and Dorofeev models. Additionally, note the
 38 improvement in the predictions for x_{DDT}/D_h Exp $<$
 39 50 when using the LM. This provides evidence of the
 40 value of simple data manipulations (e.g., non-linear
 41 regressions) to enhance the predictive capabilities of
 42 existing models and/or inform the development of
 43 new simpler expressions/correlations with compar-
 44 able or better performance. The most important as-
 45 pect is the use of large properly curated data sets cov-
 46 ering a wide range of experimental conditions, fu-
 47 els, and geometries to guide the choice of variables
 48 that explain the variance of the experimental measure-
 49 ments. Finally, additional models were also tested in
 50 this work (not shown) including but not limited to lin-
 51 ear models with dimensional variables, differentiating
 52 by BC, type of fuel, etc. However, these resulted in
 53 lower performance than the proposed NLM and LM.
 54 Strategies such as using data specific to H_2 and HC,
 55 as well as assessing kinetic mechanisms induced un-
 56 certainties were evaluated and are included as supple-
 57 mentary material for completeness.

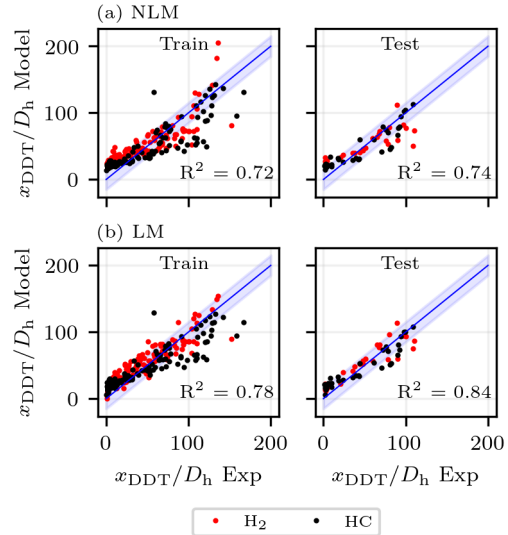


Fig. 7: a) Non-linear (NLM) and b) Logarithmic (LM) models performance for training and test data.

58 6. Conclusions

59 A large database is compiled using a comprehen-
 60 sive set of x_{DDT} data for unobstructed channels avail-
 61 able in the literature. It comprises an extensive range
 62 of experimental conditions and mixtures. The global
 63 x_{DDT} trends as a function of D_h , ϕ , and p were evalu-
 64 ated. The data shows that x_{DDT} decreases as D_h de-
 65 creases, p increases, and $\phi \rightarrow 1$. An analysis of the

1 effect of the ratios of fundamental combustion properties on x_{DDT}/D_h revealed that those that most affect
 2 it are D_h/δ_f , V_{CJ}/σ_{SL} and $\sigma - 1$. The most widely
 3 used models for x_{DDT} predictions, i.e., Silvestrini and
 4 Dorofeev, were tested against the database performing
 5 rather poorly. An update to the models constants
 6 was carried out via a non-linear least squares
 7 regression using the large database compiled. This
 8 resulted in significant improvements in their performance.
 9 Finally, two simplified models were proposed. Their
 10 predictions are significantly better than those of the
 11 original Silvestrini/Dorofeev models and higher (LM)/
 12 similar (NLM) to those obtained with the updated
 13 models. Future work will include the use of the
 14 database to: (i) train a model that will be tested on
 15 obstructed channels using an expression that captures
 16 the experimental dependence of x_{DDT} as a function of
 17 the blockage ratio; (ii) develop x_{DDT}/D_h models
 18 valid for $D_h < 3$ mm and non-unity AR channels.

20 Acknowledgments

21 The financial supports from Agence Nationale de
 22 la Recherche Program JCJC (FASTD ANR-20-CE05-
 23 0011-01), FM Global, Institut PPrime and École
 24 Doctoral MIMME are gratefully acknowledged.

25 Supplementary material

26 The following is included:

- 27 • Original Silvestrini and Dorofeev models performance
 28 against the database without performing the data
 29 pre-processing discussed in subsection 2.4.
- 30 • The updated Silvestrini and Dorofeev, and proposed
 31 NLM and LM models evaluated on different datasets:
 32 (i) against the data excluded after pre-processing,
 33 and (ii) against the H_2 and HC data separately.
- 34 • New model constants for the updated Silvestrini
 35 and Dorofeev, and proposed NLM and LM models
 36 under three scenarios: (i) without database
 37 pre-processing, (ii) using the H_2 and HC data
 38 separately from the pre-processed database, and
 39 (iii) using the pre-processed database but with
 40 different kinetic mechanisms (San Diego [44]
 41 and FFCM-2 [45]).

44 References

- 45 [1] J. Li, W. Fan, C. Yan, Q. Li, Experimental investigations
 46 on detonation initiation in a kerosene-oxygen pulse
 47 detonation rocket engine, *Combust. Sci. Technol.* 181
 48 (3) (2009) 417–432.
- 49 [2] M. Silvestrini, B. Genova, G. Parisi, F. L. Trujillo,
 50 Flame acceleration and DDT run-up distance for
 51 smooth and obstacles filled tubes, *J. Loss Prev. Process*
 52 *Ind.* 21 (5) (2008) 555–562.
- 53 [3] S. B. Dorofeev, Hydrogen flames in tubes: critical run-
 54 up distances, *Int. J. Hydrog. Energy* 34 (14) (2009)
 55 5832–5837.

- 56 [4] W. Bartknecht, Brenngas und staubexplosionen
 57 forschungsbericht f45, Bundesinstitut Fur Arbeitsschutz
 58 (Bifa), Koblenz (1971).
- 59 [5] K. Chatrathi, J. E. Going, B. Grandestaff, Flame propa-
 60 gation in industrial scale piping, *Process Saf. Prog.* 20
 61 (4) (2001) 286–294.
- 62 [6] M. Kuznetsov, V. Alekseev, I. Matsukov, S. Dorofeev,
 63 DDT in a smooth tube filled with a hydrogen–oxygen
 64 mixture, *Shock waves* 14 (2005) 205–215.
- 65 [7] M. Kuznetsov, I. Matsukov, V. Alekseev, W. Breitung,
 66 S. Dorofeev, Effect of boundary layer on flame accel-
 67 eration and DDT, in: *Proc. 20th ICDERS*, 2005.
- 68 [8] M. Kuznetsov, V. Alekseev, A. Bezmelnitsyn, W. Brei-
 69 tung, S. Dorofeev, I. Matsukov, A. Vesper, Y. G.
 70 Yankin, Report fzka-6328, Karlsruhe: Forschungszentrum
 71 Karlsruhe (1999).
- 72 [9] M. Kuznetsov et al., Evaluation of structural integrity
 73 of typical DN15 tubes under detonation loads, Report
 74 Forschungszentrum Karlsruhe (2003).
- 75 [10] R. Linds., H. Michels, Deflagration to detonation tran-
 76 sitions and strong deflagrations in alkane and alkene
 77 air mixtures, *Combust. Flame* 76 (2) (1989) 169–181.
- 78 [11] C. Proust, Gas flame acceleration in long ducts, *J. Loss*
 79 *Prev. Process Ind.* 36 (2015) 387–393.
- 80 [12] G. Thomas, G. Oakley, R. Bambrey, An experimental
 81 study of flame acceleration and deflagration to detona-
 82 tion transition in representative process piping, *Process*
 83 *Saf. Environ.* 88 (2) (2010) 75–90.
- 84 [13] R. Blanchard et al., Effect of ignition position on the
 85 run-up distance to DDT for hydrogen–air explosions,
 86 *J. Loss Prev. Process Ind.* 24 (2) (2011) 194–199.
- 87 [14] Y. Ballossier, F. Viro, J. Melguizo-Gavilanes, Flame
 88 acceleration and detonation onset in narrow channels:
 89 simultaneous schlieren visualization, *Combust. Flame*
 90 254 (2023) 112833.
- 91 [15] C. Mejia-Botero, F. Viro, J. Melguizo-Gavilanes,
 92 CH_4 - O_2 flame acceleration morphology: A compara-
 93 tive analysis under different hydrocarbon fuel, channel
 94 geometry and scale, *Proc. 29th ICDERS* (2023).
- 95 [16] K. Aizawa et al., Study of detonation initiation in hy-
 96 drogen/air flow, *Shock Waves* 18 (2008) 299–305.
- 97 [17] B. Baumann et al., On the influence of tube diameter
 98 on the development of gaseous detonation, *Zeits Elekt*
 99 *Ber der Bun phy Chem* 65 (10) (1961) 898–902.
- 100 [18] D. Pawel, P. Van Tiggelen, H. Vasatko, H. G. Wagner,
 101 Initiation of detonation in various gas mixtures, *Combust.*
 102 *Flame* 15 (2) (1970) 173–177.
- 103 [19] Y. Ballossier, Topologies de l’accélération de flammes
 104 d’ H_2 - O_2 - N_2 dans des canaux étroits: de l’allumage
 105 jusqu’à la détonation, Ph.D. thesis, ISAE-ENSMA,
 106 Poitiers (2021).
- 107 [20] J. Melguizo-Gavilanes, Y. Ballossier, L. M. Faria, Ex-
 108 perimental and theoretical observations on DDT in
 109 smooth narrow channels, *Proc. Combust. Inst.* 38 (3)
 110 (2021) 3497–3503.
- 111 [21] T. Tanaka, K. Ishii, T. Tsuboi, A study on shortening of
 112 a detonation transition distance, *Proc. Symp. Combust.*
 113 *Japanese* (2001) 461–462.
- 114 [22] L. E. Bollinger, M. C. Fong, R. Edse, Experimental
 115 measurements and theoretical analysis of detonation
 116 induction distances, *ARS J* 31 (5) (1961) 588–595.
- 117 [23] Z. Yang et al., Experimental investigation on the DDT
 118 run-up distance and propagation characteristics of deto-
 119 nation wave in a millimeter-scale spiral channel filled
 120 with hydrogen-air mixture, *Int. J. Hydrog. Energy*
 121 (2023).
- 122 [24] Z. Yang et al., Experimental study of DDT run-up dis-

- 1 tance and detonation wave velocity deficit for stoichio- 68
2 metric hydrogen-oxygen mixture in micro spiral chan- 69
3 nels, *Int. J. Hydrog. Energy* (2023). 70
- 4 [25] Y. Hsu, Y. Chao, An experimental study on flame ac- 71
5 celeration and deflagration-to-detonation transition in 72
6 narrow tubes, in: *Proc. 22th ICDERS*, 2009. 73
- 7 [26] J. Huo et al., Deflagration-to-detonation transition and 74
8 detonation propagation characteristics in a millimetre- 75
9 scale spiral channel, *Exp. Therm. Fluid Sci.* 140 (2023)
10 110773.
- 11 [27] P. Urtiew, A. Oppenheim, Experimental observations 76
12 of the transition to detonation in an explosive gas, 77
13 *Proc. Math. Phys. Eng.* 295 (1440) (1966) 13–28.
- 14 [28] M. Kuznetsov et al., Experimental study of the pre- 78
15 heat zone formation and DDT, *Combust. Sci. Technol.* 79
16 182 (11-12) (2010) 1628–1644.
- 17 [29] M. Liberman et al., On the mechanism of the 80
18 deflagration-to-detonation transition in a H₂-O₂ mix- 81
19 ture, *J. Exp. Theor. Phys.* 111 (2010) 684–698.
- 20 [30] R. Lindstedt, H. Michels, Deflagration to detonation 82
21 transition in mixtures of alkane LNG/LPG constituents 83
22 with O₂-N₂, *Combust. Flame* 72 (1) (1988) 63–72.
- 23 [31] Y. Zhao, Y. Zhang, Large eddy simulation investiga- 84
24 tion of flame acceleration and DDT of CH₄-air mixture 85
25 in rectangular channel, *Eng. Rep.* 5 (3) (2023) e12574.
- 26 [32] H. Steen, K. Schampel, Experimental investigations 86
27 on the run-up distance of gaseous detonations in large 87
28 pipes, in: *4th Int. Symp. Loss Prev. Saf. Prom. Process*
29 *Ind.*, Vol. 82, 1983, pp. E23–33.
- 30 [33] M. Wu et al., Flame acceleration and the transition to 88
31 detonation of stoichiometric C₂H₄/O₂ in microscale 89
32 tubes, *Proc. Combust. Inst.* 31 (2) (2007) 2429–2436.
- 33 [34] M. Wu et al., Transmission of near-limit detonation 90
34 wave through a planar sudden expansion in a narrow 91
35 channel, *Combust. Flame* 159 (11) (2012) 3414–3422.
- 36 [35] C.-Y. Wang, J.-K. Wang, M.-H. Wu, Visualization and 92
37 parametric study of reaction propagation in meso-scale 93
38 tubes, in: *ASME*, Vol. 43765, 2009, pp. 265–271.
- 39 [36] J. Li, P. Zhang, L. Yuan, Z. Pan, Y. Zhu, Flame 94
40 propagation and detonation initiation distance of ethy- 95
41 lene/oxygen in narrow gap, *Appl. Therm. Eng.* 110 96
42 (2017) 1274–1282.
- 43 [37] J. Finigan et al., Deflagration-to-detonation transition 97
44 via the distributed photo ignition of carbon nanotubes 98
45 suspended in fuel/oxidizer mixtures, *Combust. Flame* 99
46 159 (3) (2012) 1314–1320.
- 47 [38] F. Pintgen, Z. Liang, J. Shepherd, Structural response 100
48 of tubes to deflagration-to-detonation transition, in:
49 *Proc. 21th ICDERS*, 2007, pp. 23–27.
- 50 [39] M. Liberman et al., Deflagration-to-detonation transi- 101
51 tion in highly reactive combustible mixtures, *Acta As-*
52 *tronaut.* 67 (7-8) (2010) 688–701.
- 53 [40] J. Li, W.-H. Lai, K. Chung, Tube diameter effect 102
54 on deflagration-to-detonation transition of propane- 103
55 oxygen mixtures, *Shock waves* 16 (2006) 109–117.
- 56 [41] Z. Pan, Z. Zhang, P. Zhang, Effects of a significant 104
57 boundary layer on the flame acceleration and transition 105
58 to detonation in millimeter-scale tubes, *Aerosp. Sci.*
59 *Technol.* 126 (2022) 107533.
- 60 [42] H.-W. Ssu, M.-H. Wu, Formation and characteristics of 106
61 composite reaction–shock clusters in narrow channels,
62 *Proc. Combust. Inst.* 38 (3) (2021) 3473–3480.
- 63 [43] F. Pedregosa et al., Scikit-learn: Machine learning in 107
64 Python, *J. Mach. Learn. Res.* 12 (2011) 2825–2830.
- 65 [44] F. Williams, Chemical-kinetic mechanisms for combus- 108
66 tion applications. san diego mechanism web page, me-
67 chanical and aerospace engineering (combustion re-
68 search), university of california at san diego (2022).
- [45] Y. Zhang, W. Dong, R. Xu, G. P. Smith, H. Wang,
Foundational fuel chemistry model 2-iso-butene
chemistry and application in modeling alcohol-to-jet
fuel combustion, *Combustion and Flame* 259 (2024)
113168.